Journal of Research and Applications in Mechanical Engineering
ISSN: 2229-2152 (Print); 2697-424x (Online)
(2025) Vol. 13, No. 2, Paper No. JRAME 25-13-022
[DOI: 10.14456/jrame.2025.22]

Research Article

Enhancing Combustion Analysis: Implementation and Validation of Laminar Premixed Methane-Air Jet-Impinging Flame Simulation in OpenFOAM

P. Kamma[1,5]
K. Loksupapaiboon[2, 5]
J. Phromjan[3, 5]
C. Suvanjumrat[4, 5,*]
[1] *Department of Mechanical and Manufacturing Engineering, Faculty of Science and Engineering, Kasetsart University, Chalermphrakiat Sakon Nakhon Province Campus, Sakon Nakhon 47000, Thailand*
[2] *Department of Maritime Engineering, Faculty of International Maritime Studies, Kasetsart University Sriracha Campus, Chonburi 20230, Thailand*
[3] *Department of Mechanical Engineering, Faculty of Engineering, King Mongkut's University of Technology Thonburi, Bangmod, Bangkok 10140, Thailand*
[4] *Department of Mechanical Engineering, Faculty of Engineering, Mahidol University, Salaya, Nakhon Pathom 73170, Thailand*
[5] *Laboratory of Computer Mechanics for Design (LCMD), Department of Mechanical Engineering, Faculty of Engineering, Mahidol University, Salaya, Nakhon Pathom 73170, Thailand*

Received 13 September 2024
Revised 31 October 2024
Accepted 5 November 2024

Abstract:
This research utilized the open-source toolbox OpenFOAM to conduct a numerical investigation of the laminar premixed methane-air jet-impinging flame. OpenFOAM, a software based on computational fluid dynamics (CFD) and employing the finite volume method (FVM), was used to perform transient simulations with a chemically compressible reacting flow model integrated with a conjugated heat transfer model. Key parameters such as burner-to-plate distances (H/d = 0.04 and 0.06 m), mixture equivalence ratios (ϕ = 0.8-2.0), and Reynolds numbers (Re = 500, 750 and 1,000) were varied to thoroughly examine their effects. The simulated results were rigorously validated against experimental data from previous research, focusing on flame height and thermal efficiency, which are critical parameters in the jet-flame impinging system. The validation demonstrated a strong correlation, confirming the accuracy and reliability of the simulations. This alignment underscores the usefulness of the modeling approach and highlights the potential of using OpenFOAM for detailed combustion studies, paving the way for future research and optimization in this field.

Keywords: *CFD, Combustion, Impinging flame, Laminar methane-air flame, OpenFOAM*

1. Introduction

The impinging premixed jet flame system is a high-performance direct flame heating system widely utilized in both household and industrial applications due to its high heat transfer rate, appealing aesthetics, ease of operation, and low pollution emissions. These systems operate effectively across various pressures and use hydrocarbon gaseous fuels, such as natural or liquefied petroleum gas, for premixed combustion. A thorough understanding of their behavior is essential for optimizing combustion system design and enhancing energy efficiency.

* Corresponding author: C. Suvanjumrat
E-mail address: chakrit.suv@mahidol.ac.th

The configuration of the impinging premixed jet flame system involves mixing gaseous fuel with an oxidizer, typically ambient air, within the burner prior to ejection. Burners may feature a single port, like a Bunsen burner, or multiple ports, as seen in domestic stoves. The resulting gaseous mixture, referred to as reactants, is ignited to form a flame consisting of two parts: the conical premixed flame and the diffusion flame outside the cone. The diffusion flame impinges on the top wall, with its alignment either normal or oblique to maximize heat transfer. The flow within the system can be divided into the free jet and stagnation point zone—where jet velocity drops to zero and heat flux peaks—and the wall jet region, where the velocity runs predominantly parallel to the impinging wall [1].

The thermal efficiency of an impinging premixed jet flame system, which reflects its energy performance and the effectiveness of fuel-to-heat conversion, is a key quality indicator. Numerous experimental and computational studies have investigated parameters influencing this efficiency, providing insights critical for system optimization [2, 3]. Among these parameters, flame height and shape are particularly vital for optimizing system performance. Proper flame positioning ensures that maximum heat release and temperature are directed toward the target impinging plate, thereby achieving optimal thermal efficiency. Research indicates that the optimal position is typically slightly away from the premixed flame surface, although this can vary with other factors [4]. Accordingly, studies have focused on optimizing the burner-to-plate distance (H/d), a dimensionless parameter that relates the distance from the burner exit to the target plate (H) to the nozzle diameter (d), to achieve precise flame arrangement for enhanced heat transfer.

Prior research has emphasized the impact of parameters such as fuel composition, Reynolds number (Re), and equivalence ratio on flame structure and height, which are closely associated with H/d [2]. The heat produced by the flame is strongly linked to the fuel's heating value, and efforts to optimize combustion processes while promoting zero-carbon energy resources have led to the incorporation of environmentally friendly fuels, such as hydrogen and ammonia, to enrich traditional hydrocarbon fuels [5]. These modifications alter flame structure and height due to changes in flame speed. Adjustments in the equivalence ratio also significantly influence flame height. While the flame typically maximizes heat release near the stoichiometric condition due to complete combustion, lean or rich flames, which are generally taller, may yield lower heat transfer rates [6]. This occurs because the entrainment of environmental air results in lower temperatures beneath the target-impinging plate. Additionally, increasing Re generally elevates flame height, temperature, and heat flux on the impinging plate; however, excessively high Re can cause the premixed flame cone to contact the impinging plate, leading to cooling effects due to unburned reactants [7]. Other factors, such as ambient air velocity, burner nozzle type, and nozzle alignment, may also affect the heating system but are considered minor and beyond the scope of this study.

To deepen the understanding of complex dynamics within impinging premixed jet flame systems, numerical simulations offer a cost-effective alternative to complex experimental approaches. This study leverages computational fluid dynamics (CFD) to model the combustion process, effectively capturing the coupled effects of fluid flow and chemical reactions. While commercial CFD tools are widely utilized due to their strong alignment with experimental results [8], this research circumvents the high costs associated with proprietary software by utilizing OpenFOAM. Although OpenFOAM provides significant flexibility, its application in examining the thermal characteristics and efficiency of jet-impinging flames remains limited. Through its capacity for customized solvers and boundary conditions, OpenFOAM facilitates detailed analysis of laminar flame dynamics, employing complex reacting flow models and conjugate heat transfer, thus establishing it as a robust tool for advanced combustion research [9, 10].

In this study, the implemented models account for variations in key parameters, including mixture equivalence ratios (Phi = 0.8–2.0), burner-to-plate distances (H/d = 4 and 6), and mixture Reynolds numbers (Re = 500, 750 and 1,000). These parameters were subjected to rigorous numerical analysis to capture the full scope of their impact on flame behavior and thermal efficiency. The simulated results were then meticulously validated against the experimental data provided by Pramod Kuntikana et al. [6], ensuring a high degree of accuracy and reliability. This comprehensive validation not only confirms the efficacy of the developed model but also highlights its potential as a cost-effective and broadly applicable tool for studying similar combustion systems. The outcomes of this research contribute valuable insights into the optimization of impinging premixed jet flame systems, offering a solid foundation for future investigations and practical applications in both industrial and domestic settings.

2. Numerical Models

In this study, the laminar impinging flame was simulated using chtMultiRegionFoam, an OpenFOAM solver based on Computational Fluid Dynamics (CFD) and the Finite Volume Method (FVM). This solver is specifically designed to manage steady and transient compressible flows alongside solid heat conduction. It also facilitates conjugate heat transfer between different regions, accounting for buoyancy effects, turbulence, chemical reactions, and radiation modeling. In the fluid region, the governing equations within this solver, expressed in a conservative formulation, include the continuity, momentum, species mass fraction, and energy equations. These are outlined as follows [11]

Continuity:

$$\frac{\partial \rho}{\partial t} + \nabla \cdot (\rho U) = 0 \tag{1}$$

Momentum:

$$\frac{\partial}{\partial t}(\rho U) + \nabla \cdot (\rho U U) = -\nabla \mathrm{p} + \nabla \tau \tag{2}$$

Species mass fraction:

$$\frac{\partial}{\partial t}(\rho Y_k) + \nabla \cdot (\rho U Y_k) + \nabla \cdot \dot{J}_k = \dot{\omega}_k \tag{3}$$

Energy:

$$\frac{\partial \rho}{\partial t}(\rho h_s) + \nabla\left(\frac{\rho}{U h_s}\right) + \frac{\partial}{\partial t}(\rho K) + \nabla(\rho U K) = \nabla\left(\frac{\lambda}{C_p}\nabla h_s\right) + \dot{Q} + \nabla\left(\rho \sum_{k=1}^{N} \nabla h_k \dot{J}_k\right) + \frac{\partial p}{\partial t} + S_e \tag{4}$$

where t, ρ, U, p, τ, Y_k, $\dot{J}_k$, $\dot{\omega}_k$, h_s, K, λ, C_p, $\dot{Q}$, h_k and S_e represent the time, reacting mixture density, velocity, pressure, viscous stress tensor (excluding bulk viscosity), mass fraction of species k, production rate of species k due to chemical reaction, sensible enthalpy, kinetic energy, thermal conductivity, heat capacity at constant pressure, heat release rate from chemical reaction, specific enthalpy of species k, and the energy source term, respectively. Radiative heat transfer is calculated using the P1 radiation model, which is integrated via this source term.

Additionally, in the solid region, only the energy equation needs to be solved as follows [12]

$$\frac{\partial \rho}{\partial t}(\rho h_s) = \nabla\left(\frac{\lambda}{C_p}\nabla h_s\right) \tag{5}$$

The above expression indicates that the rate of change in enthalpy is equivalent to the divergence of the heat conducted within a solid region. At the interface where the fluid and solid regions converge, there is a coupling wherein the temperatures of both phases are equal. This relationship implies that the heat flux (Q) entering one region from one side of the interface must be equal to the heat flux exiting the other region on the opposite side of the domain. The expression can be written as:

$$Q_{fluid} = -Q_{solid} \tag{6}$$

To solve the governing equations, The PIMPLE algorithm was employed, which integrates the PISO (Pressure Implicit with Splitting of Operator) and SIMPLE (Semi-Implicit Method for Pressure-Linked Equations) algorithms to address the pressure-velocity coupling problem. For methane-air combustion simulations, a reduced reaction mechanism comprising 25 species and 132 reactions was utilized, specifically designed for modeling laminar methane-air premixed flames [13]. Finite rate chemistry with Arrhenius reaction rates was used to estimate the chemical formation rate during combustion. A state-of-the-art model for simulating diffusion flux in detailed laminar

premixed combustion was implemented and validated [11, 14], thereby avoiding the computational overhead associated with multicomponent diffusion and mixture-averaged models [11]. Furthermore, the computation was accelerated by the Tabulation Dynamics Adaptive Chemistry algorithm [14], which dynamically adjusts the chemical kinetics based on local flow conditions and utilizes precomputed lookup tables for efficient simulations. Computational stability was ensured by employing the Courant number (Co) to assess time step requirements throughout the simulation.

Numerical discretization relied on OpenFOAM schemes. Temporal discretization employed the transient bounded first-order Euler scheme. Gradient and Laplacian terms were addressed using Gauss integration with the second-order central differencing scheme for interpolating values between cell centers and faces. Divergence terms were integrated using Gauss integration, while the linearUpwind scheme was used for interpolation, incorporating an upwind weighting factor and an explicit correction based on the local cell gradient. The geometric-algebraic multi-grid method (GAMG) was used for pressure, while other variables were solved using the preconditioned bi-conjugate gradient stabilized method (PBiCGStab), with all tolerances set to 10^{-7}. Specific details for each case are provided in the subsequent sections.

3. Impinging flame modeling

The experimental setup conducted by Pramod Kuntikana et al. [6] was utilized to establish the CFD laminar impinging flame model in this study. Their research focused on analyzing the thermal characteristics of impinging laminar premixed methane-air flames, examining variations in Reynolds numbers, equivalence ratios, and the distances between the burner and the impinging plate. These variations were ultimately quantified in terms of thermal efficiency. Additionally, their findings indicated that the position of the premixed flame front had a significant impact on thermal efficiency. Consequently, the vertical position of the premixed flame front and the associated thermal efficiency served as valuable benchmarks for validating our CFD code.

3.1 Impinging flame configuration

According to the experiment [6], the burner tube had a diameter of 10 mm and a thickness of 0.0005 m, and it ejected the reacting mixture at three different Reynolds numbers: 500, 750 and 1000. The mixture, consisting of methane and air, was tested with equivalence ratios ranging from 0.8 to 2.0. The experiment utilized a square plate with dimensions 0.15 m × 0.15 m × 0.001 m as the impinging plate, with two different burner-to-plate distances, H/d: 0.04 m and 0.06 m.

3.2 Computational model and Boundary condition

For the CFD simulation, the computational domain was simplified to a two-dimensional axisymmetric configuration, as shown in Figure 1(a). To accurately capture the impact of heat transfer between the flame and the wall, including the burner tube and the impinging plate, we employed a conjugate heat transfer model. This model explicitly calculates the wall temperature by evaluating heat transfer from the fluid (flame) to the solid. It incorporates a solid domain, including the burner tube with a thickness of 0.0005 m, along with a fluid domain. To specifically address heat transfer at the impinging plate wall, half of the impinging plate, with a radius of 0.075 m, was considered the domain radius, neglecting lateral heat transfer within the plate. Vertically, the domain extended from the burner exit to distances corresponding to H/d values of 0.04 and 0.06 m. Additionally, a section of the tube beneath the burner exit was included to ensure a fully developed incoming flow, thereby minimizing the influence of boundary conditions on the flame. This configuration was designed to account for the effect of the burner tube wall on the flame. Furthermore, the length of the burner tube was varied in subsequent sections to identify the optimal conditions for simulation.

Boundary conditions for the fluid domain were defined using a computed Poiseuille solution to establish a fully developed velocity profile. Inlet values for velocity, species mass fractions, and a uniform temperature of 298 K were specified based on the Reynolds numbers and equivalence ratios. At the outlet, OpenFOAM's pressureInletOutletVelocity condition was applied for velocity, while temperature and species mass fractions were set using the inletOutlet condition to ensure zero gradients for outgoing flow and fixed/computed values for incoming flow. The burner tube and impinging plate were assigned a no-slip velocity condition, with a zero-gradient for mass fractions, and the impinging wall temperature was set at 403 K, corresponding to the boiling point of water [15].

A wedge boundary condition was applied on the side faces to treat the axisymmetric domain as two-dimensional. The pressure was set to zero-gradient across surfaces, with a fixed value of 1 atm at the outlet. Initial conditions across the domain included 298 K, 1 atm, and standard air mass fractions. A summary of these boundary conditions is provided in Table 1.

For the solid domain, heat transfer from the fluid to the solid at the interface was managed using the turbulentTemperatureRadCoupleMixed boundary condition provided by OpenFOAM. On the external face of the solid, heat loss due to convection and radiation was considered. A convective heat transfer coefficient of 5 W/m²·K and an emissivity coefficient of 0.95 were used for these calculations. The thermal properties of the solid domain were set to those of standard carbon steel, with a thermal conductivity of 45 W/m·K, a density of 7,800 kg/m³, and a specific heat capacity of 465 J/kg·K. The initial temperature of the solid was set to match the ambient air temperature. The computational simulation began with solving the cold flow of the unburned reacting mixture introduced into the domain. After several thousand iterations, equivalent to 0.3 seconds of simulation time, the reacting mixture had filled the domain. Subsequently, ignition was achieved using an explicit heat source, with a temperature of 2000 K applied to certain grids above the burner for a brief period of 0.01 seconds. This procedure activated the volumetric reaction and energy equations, which were coupled and computed. The simulation continued until it reached a total time of 5.0 seconds, at which point the flame had reached a statistically steady state.

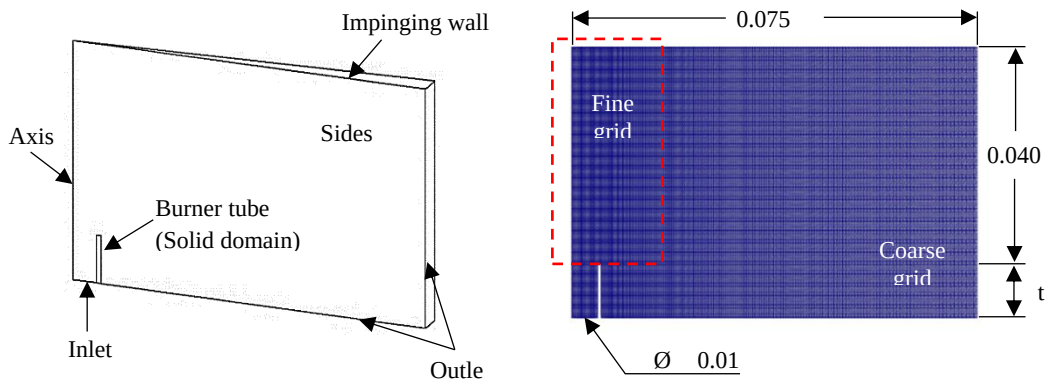

(a) Geometrical model

(b) Computational domain with grid structure shown for the fluid domain only.

Fig. 1. Computational domain

Table 1: Boundary condition specifications for jet-impinge flame simulations.

Boundary	Fields			
	u	**p**	**T**	**Y**
Inlet	fixedValue	zeroGradient	fixedValue	fixedValue
Outlet	pressureInletOutletVelocity	inletOutlet	inletOutlet	zeroGradient
Impinging Wall	noSlip	fixedValue	fixedValue	zeroGradient
Sides	wedge	wedge	wedge	wedge

4. Result and Discussion

4.1. Computational grid and independence test

The geometric model and grid resolution were established using OpenFOAM's BlockMesh utility. A uniform fine grid, with equal spacing of Δx and Δy, was applied to the flame zone, delineated by the red dashed line in Figure 1(b). Outside this fine block, a coarser grid with a proportional growth rate of 1.2 was used to minimize the total grid count and expedite the computational process.

A grid-independence analysis was performed to assess the impact of grid resolution on the computational solution. The simulation model an H/d of 0.04 m with a burner tube length (tD) of 2D (0.005 m). The test, conducted under

stoichiometric conditions with an equivalence ratio and Reynolds number of 500, used an inlet velocity of 0.81 m/s, calculated from the mixture density and dynamic viscosity [8]. This velocity, along with mass fractions of 0.055 for CH_4, 0.725 for O_2 and 0.220 for N_2, was applied at the inlet boundary with a pressure of 1 atm. Five distinct grid resolutions were employed, with fine grid sizes at the flame zone of 0.15, 0.20, 0.25, 0.50 and 1.0 mm, resulting in total grid counts of 71,336, 38,804, 24,708, 8,330 and 1,584 respectively. Each grid resolution was labeled as Grid1 through 5.

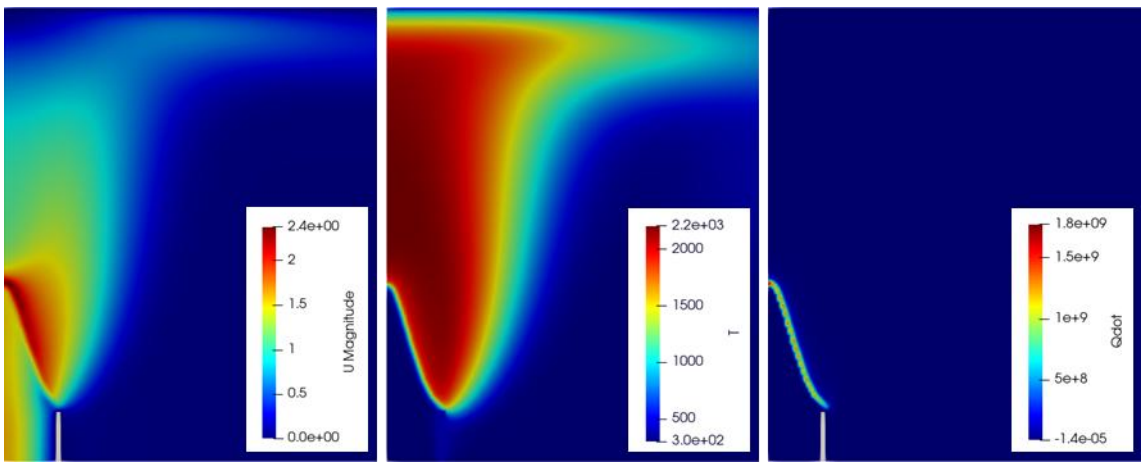

(a) Velocity (b) Temperature (c) Heat release rate

Fig. 2. Computational results in the fluid domain.

Figures 2(a), (b) and (c) present the computational results for premixed flame velocity, temperature, and heat release rate, respectively, using the grid resolution of Grid3. These contours depict a semi-conical shape known as the premixed cone. In the velocity contour (Figure 2(a)), the incoming reactants flow from the inlet into the domain, with the velocity gradient illustrating a fully developed distribution inside the burner tube. The velocity peaks at the premixed cone due to intense combustion within the unburned mixture, with the rapid expansion of hot gases leading to elevated velocities. Surrounding the premixed cone, the velocity decreases due to lower combustion rates and the influx of environmental air, with the stagnation point occurring at the impinging plate surface where the fluid velocity drops to zero.

In the temperature contour (Figure 2(b)), the premixed cone contains low-temperature unburned reactants, while outside it, temperatures exceed 2,000 K, indicating combusted gas. Far from the outer cone, the temperature is diluted by fresh air. The heat release rate contour (Figure 2(c)) identifies regions of intense chemical reaction and heat release, aligning with the premixed cone. This contour effectively indicates the reaction zone and flame height [13], which are crucial for evaluating the heat transfer system. The premixed flame height was used to assess grid resolution.

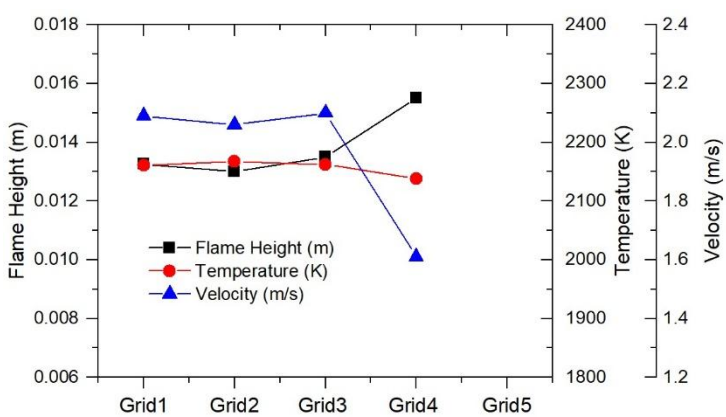

Fig. 3. Computed temperature, velocity, and flame height for varying grid resolutions.

Figure 3 presents the computational results, including temperature, velocity, and heat release rate height (flame height), from numerical simulations across different grid resolutions. For Grid1, Grid2 and Grid3, the flame height remains consistent at approximately 0.013 m, with an error of less than 2% compared to the finest grid (Grid1). In Grid4, the flame height measures 0.0155 m, resulting in an error of about 14%. In Grid5, the flame extinguishes after a few simulation steps, highlighting the importance of utilizing fine grid sizes and conducting grid independence testing in chemically reacting flow modeling. Consequently, the grid resolution of Grid3 (0.25 mm for the fine grid) was determined to be reliable for accurate simulations without incurring excessive computational time.

4.2 Length of burner tube

This section examines the impact of varying burner tube length (tD) on computational outcomes. To reduce the computational load associated with longer tD values, we use the Poiseuille solution for the incoming flow, ensuring a fully developed velocity profile and allowing for a significant reduction in tD. The analysis includes five CFD configurations (Case 1 to Case 5) with a consistent H/d of 0.04 m and tD values of 0D, 0.5D, 1D, 3D and 5D, where "D" represents the burner diameter. Initial and boundary conditions align with those used in the prior grid-independence tests. In the 0D scenario, the burner tube wall is omitted, leaving only the burner rim at a constant temperature of 350 K [16], and the conjugate heat transfer model is deactivated.

Figure 4(a) compares the velocity profile at 10 mm above the burner exit. All cases exhibit a consistent trend: a uniform velocity near the flow center (0-1 mm), a sharp increase to the maximum velocity at the premixed cone, and a subsequent decrease to zero in the surrounding air. Variations in tD result in distinct differences in velocity profiles. Case 1 shows the highest velocity, with longer tD values leading to a reduction in velocity. This trend is also reflected in Figure 4(b) for flame height, where Case 1 has the tallest flame compared to Cases 2-5.

Figure 5 compares radial temperature and density plots at the burner exit for different tD values. In Case 1 (without tD), there is no conjugate heat transfer between the flame and the burner tube wall, resulting in a constant temperature (298 K) and density (1.115 kg/m^3), with no preheating of the unburned reactant. In Cases 2-5, conjugate heat transfer is included, transferring heat from the flame to the burner tube wall via convection and radiation. This preheats the unburned reactants near the tube wall (approximately 0.005 m), while those near the center of the flow are minimally affected, as shown in Figure 5. The increased wall temperature lowers the density near the wall, affecting the incoming fluid velocity. With increasing tD, the temperature and density gradients become less steep, impacting computational accuracy since reactant temperature and density are crucial for flame speed calculations. This demonstrates that models with different tD values produce varying results for velocity and flame height, as illustrated in Figures 4 and 5.

Figures 4 and 5 indicate that increasing tD does not necessarily yield more accurate results and only increases computational costs. Moreover, there is an insignificant difference between the results of Cases 4 and 5. Therefore, Case 4, with a tD of 3D, is considered the most reliable for simulation.

4.3 Flame height

As discussed in the preceding section, the height of the premixed cone flame is a critical factor influencing the heat transfer characteristics of the impinging configuration. To achieve optimal heat flux distribution, the flame tip should be positioned in close proximity to the impinging surface. Consequently, the simulated height of the premixed cone was validated by comparing it with the visible flame height measured by [14]. Cases where the unburned premixed cone either contacts or submerges into the impinging surface, leading to insufficient heat transfer, were excluded from this comparison. Furthermore, the validation cases were selected based on available experimental data.

Figure 6(a)-(e) presents a comparative analysis of the simulated and measured heights of the premixed cone. Figures 6(a)-(c) depict the results for an H/d ratio of 0.4 m, corresponding to Reynolds numbers of 500, 750 and 1000, respectively. Figures 6(d)-(f) display the results for an H/d ratio of 0.6 m, corresponding to Reynolds numbers of 500, 750 and 1000, respectively. The comparative analysis indicates that all cases align with the experimental flame height measurements.

The findings reveal that the Reynolds number (Re) significantly influences the heat transfer characteristics of the impinging flame jet. As fluid dynamics principles suggest, higher Re values increase flow velocity and turbulence,

thereby intensifying convective heat transfer. With rising Re, the premixed flame cone moves closer to the impinging surface, which boosts heat release and heat flux near the surface, leading to an enhanced overall heat transfer rate. This underscores the importance of optimizing Re in applications requiring precise thermal control, such as combustion chambers and industrial heating systems.

Conversely, the H/d ratio has minimal impact on flame height within the tested range, indicating it does not significantly alter flame structure or heat distribution. As a result, adjusting the H/d ratio may yield limited improvements in heat transfer efficiency compared to modifications in Re. These findings emphasize the need to prioritize Re control over H/d adjustments to optimize heat transfer in jet-impinging systems.

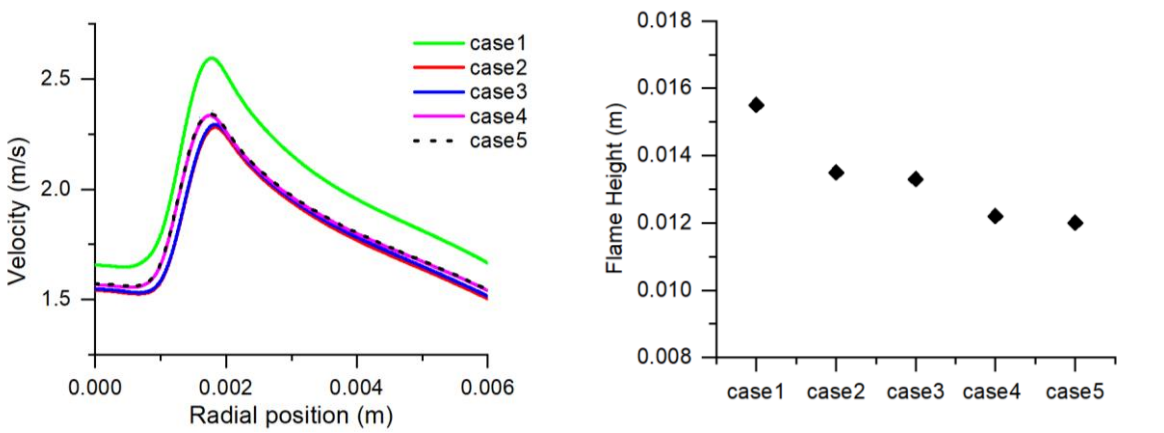

(a) Radial plot of velocity profile 10 mm above the burner exit

(b) Flame height

Fig. 4. Comparison of radial plots for different burner tube lengths.

4.4 Thermal efficiency

In this section, the validation of simulated impinging flame results is evaluated based on thermal efficiency (η_{th}), benchmarked against values from [6]. The benchmark efficiency was derived using experimental data obtained through the steady wall heat flux technique, which integrates combustion and heat transfer efficiencies to determine thermal efficiency. In contrast, this study employs transient simulations, allowing for a time-resolved analysis of wall heat flux variations on the impinging surface, as illustrated in Figure 7.

Initially, the wall heat flux is negative due to the constant-temperature condition applied to the impinging wall, causing heat to transfer from the boundary into the cooler domain. During this period, fresh reactants are introduced from the burner, with ignition occurring around 0.3 seconds. Subsequent combustion releases heat, leading to a sharp increase in wall heat flux. By approximately 3 seconds, the wall heat flux stabilizes, reaching a statistically steady state that allows for the calculation of an averaged wall heat flux value to evaluate thermal efficiency. This averaged thermal efficiency is then compared to the benchmark efficiency derived from experimental data as follows:

$$\eta_{th} = \frac{q''_{sim}}{q''_f} \tag{7}$$

where q''_{sim} represents the wall heat flux computed by the conjugated heat transfer model. q''_f represents the maximum heat release rate from fuel, computed based on higher heating value and mass flow rate.

Figure 8(a)-(e) demonstrates a consistent agreement between the simulated and measured thermal efficiency of the premixed cone. Figures 8(a)-(c) show the results for an H/d ratio of 0.4 m, corresponding to Reynolds numbers (Re) of 500, 750 and 1000, respectively. Figures 8(d)-(f) present the results for an H/d ratio of 0.6 m, also corresponding to Reynolds numbers of 500, 750 and 1000, respectively.

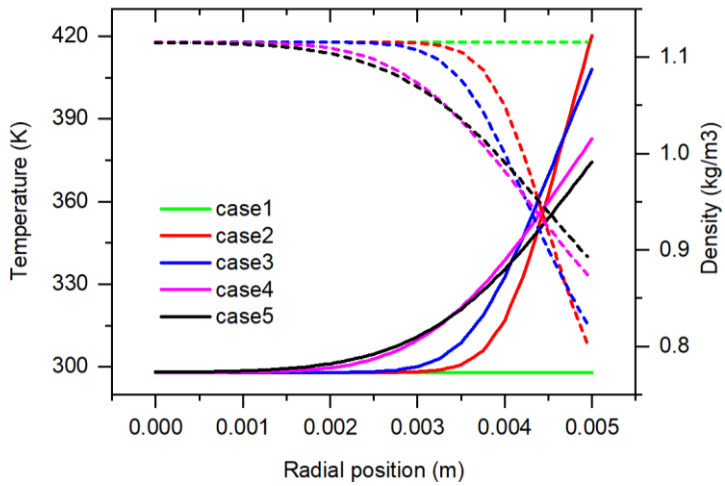

Fig. 5. Comparison of radial plots for different burner tube lengths: Solid lines indicate gaseous temperature and dashed lines represent density.

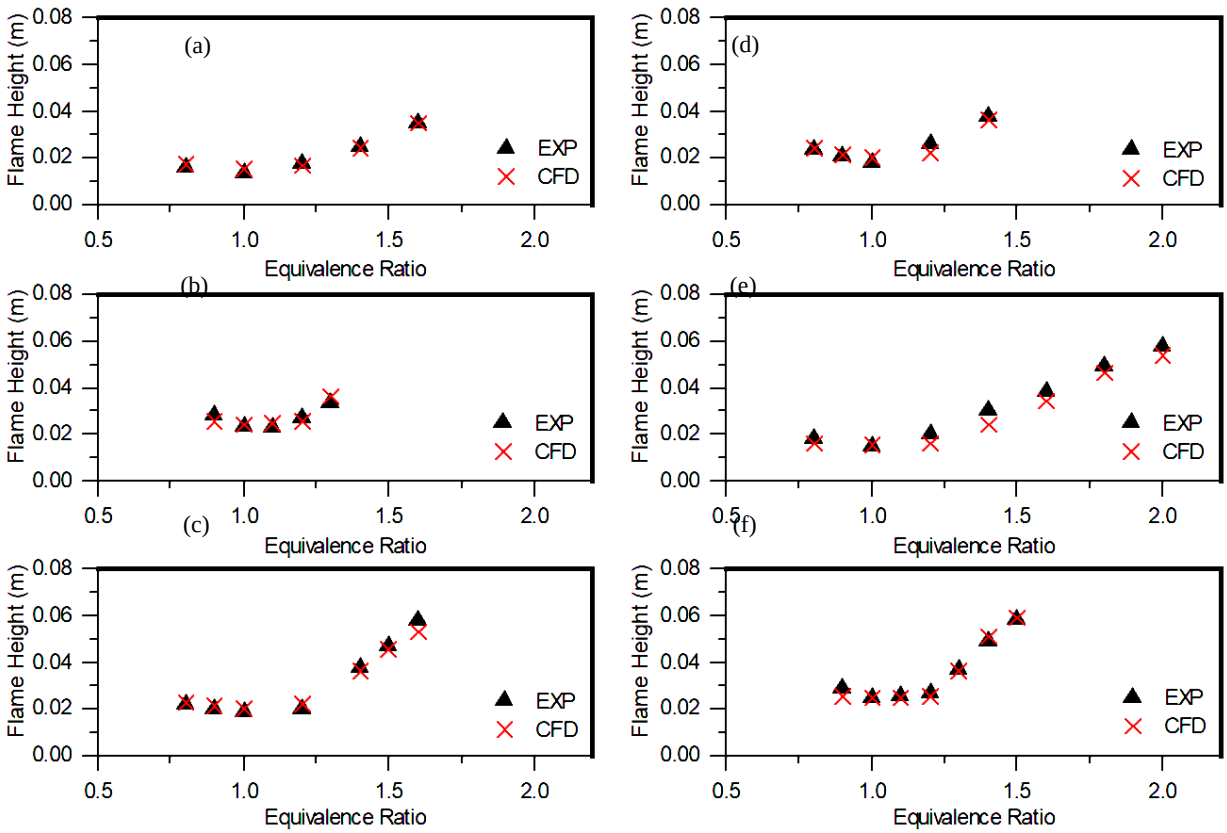

Fig. 6. Comparison of simulated and measured premixed cone heights: (a)-(c) H/d = 4 with Reynolds numbers of 500, 750 and 1000, (d)-(f) H/d = 6 with Reynolds numbers of 500, 750 and 1000.

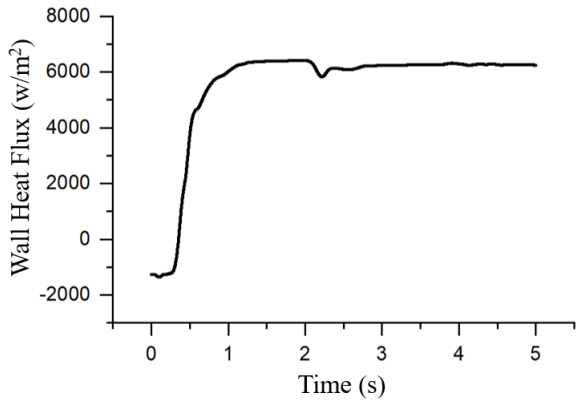

Fig. 7. Time-dependent variation of wall heat flux on the impinging surface, simulated at Re = 500, ϕ = 1.2 and HT = 0.6.

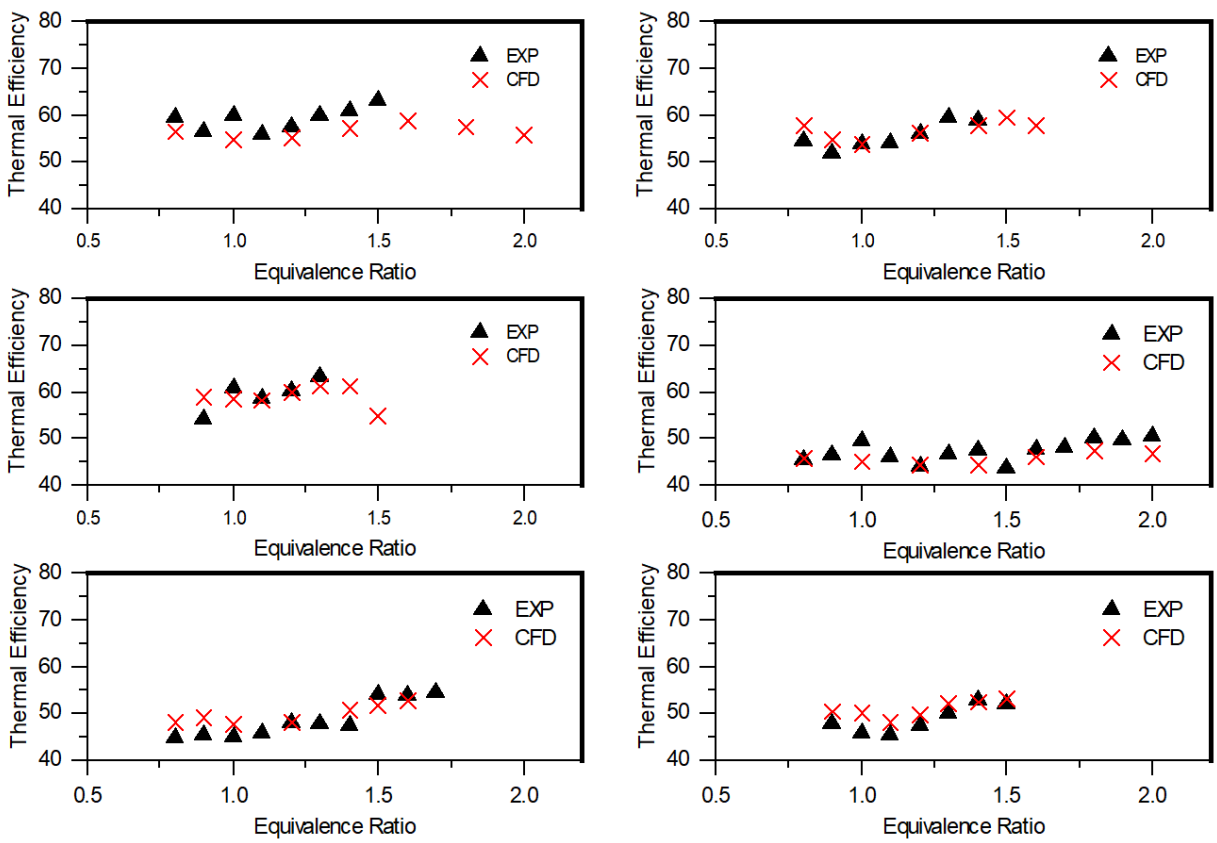

Fig. 8. Comparison of simulated and measured flame thermal efficiency: (a)-(c) H/d = 4 with Reynolds numbers of 500, 750 and 1000; (d)-(f) H/d = 6 with Reynolds numbers of 500, 750 and 1000.

5. Conclusion

This study demonstrates the effectiveness of Computational Fluid Dynamics (CFD) in assessing the thermal efficiency of impinging flame systems, offering a practical and cost-effective alternative to traditional experimental methods. By employing the ChtMultiRegionFOAM solver within OpenFOAM, we were able to accurately model the interaction between laminar premixed flames and their surrounding walls through a conjugate heat transfer approach.

The CFD domain was meticulously designed to mirror the experimental setup reported in the literature, ensuring relevant and reliable results. Key findings of this study are

1. Model Accuracy: The ChtMultiRegionFOAM solver proved highly effective in simulating the dynamics of laminar premixed flames interacting with solid boundaries. The results from our simulations align closely with experimental data, demonstrating accurate predictions of flame shape, premixed cone height, and thermal efficiency (η_{th}) across a range of equivalence ratios (ϕ) and Reynolds numbers (Re). This agreement underscores the solver's capability in capturing the complex thermal and flow phenomena involved.

2. Grid Resolution: The necessity for a fine grid in modeling chemically reacting flows was evident. Our grid independence study highlighted that using a sufficiently fine grid is critical for capturing the nuances of the flow and thermal interactions accurately. The findings advocate for rigorous grid independence testing to ensure the precision and reliability of CFD simulations.
3. Conjugate Heat Transfer: The impact of conjugate heat transfer at the burner rim emerged as a significant factor influencing flame height and thermal efficiency. Accurate simulation of these parameters requires careful consideration of heat transfer between the flame and the burner tube. The results indicate that incorporating conjugate heat transfer is essential for correctly predicting reactant velocity, density, and premixed cone height, all of which affect overall thermal efficiency.

4. Burner Tube Length: Our analysis revealed that the length of the burner tube (tD) plays a crucial role in the simulation's accuracy. Specifically, employing the Poiseuille solution for a fully developed velocity profile, we found that the burner rim length should be a minimum of three times the burner diameter to effectively mitigate non-uniform flow effects and ensure reliable heat transfer modeling. This recommendation helps in achieving accurate flame height and thermal efficiency predictions.

5. This CFD code is currently validated only for laminar methane-air premixed flame conditions. When applied to other systems, such as those involving different fuels, it requires thorough evaluation and validation of the corresponding reaction mechanisms. Additionally, the code does not support turbulent flow, necessitating substantial modifications to simulate turbulent combustion accurately. Acknowledging and addressing these limitations is essential for expanding the code's applicability to diverse contexts within combustion research.

Overall, this study validates the use of advanced CFD techniques for modeling and optimizing impinging flame systems, providing valuable insights into the design and operational parameters necessary for enhancing thermal efficiency in practical applications.

References

[1] Schuhler E, Lecordier B, Yon J, Godard G, Coppalle A. Experimental investigation of a low Reynolds number flame jet impinging flat plates. Int J Heat Mass Transf. 2020;156:119856.

[2] Gao W, Hu W, Yan R, Yan W, Yang M, Miao Q, Yang L, Wang Y. Comprehensive review on thermal performance enhancement of domestic gas stoves. ACS Omega. 2023;8(30):26663–26684.

[3] Namkhat A, Jugjai S. Prediction of total equivalence ratio for a self-aspirating burner. J Res Appl Mech Eng. 2018;1(2):31–36.

[4] Wei ZL, Zhen HS, Leung CW, Cheung CS, Huang ZH. Heat transfer characteristics and the optimized heating distance of laminar premixed biogas–hydrogen Bunsen flame impinging on a flat surface. Int J Hydrogen Energy. 2015;40(45):15723–15731.

[5] Berwal P, Khandelwal B, Kumar S. Effect of ammonia addition on laminar burning velocity of CH_4/H_2 premixed flames at high pressure and temperature conditions. Int J Hydrogen Energy. 2024;49(part B):112–125.

[6] Kuntikana P, Prabhu S. Impinging premixed methane–air flame jet of tube burner: thermal performance analysis for varied equivalence ratios. Heat Mass Transf. 2019;55:18–19.

[7] Zhen HS, Chen KD, Chen ZB, Wei ZL, Fu LR. Heat transfer analysis of impinging flames using field synergy principle. Case Stud Therm Eng. 2023;43:102807.

[8] Hua J, Pan J, Li F, Baowei F, Li Z, Ojo AO. Heat transfer characteristics of premixed methane–air flame jet impinging on a hemispherical surface. Fuel. 2023;343:127698.

[9] Threepopnartkul K, Suvanjumrat C. The effect of baffles on fluid sloshing inside the moving rectangular tank. J Res Appl Mech Eng. 2018;1(2):37–42.
[10] Chaichanasiri E, Suvanjumrat C. Simulation of three-dimensional liquid-sloshing models using C++ open source code CFD software. Kasetsart J Nat Sci. 2012;46(6):978–995.
[11] Kamma P, Suvanjumrat C. A novel diffusion flux modeling for laminar premixed flame simulation with OpenFOAM. Results Eng. 2023;20:101462.
[12] Chokngamvong S, Suvanjumrat C. Development of conjugate heat- and moisture-transfer model for pineapple drying using OpenFOAM. Case Stud Therm Eng. 2024;60:104770.
[13] Kamma P, Promtong M, Suvanjumrat C. Development of a reduced mechanism for methane combustion in OpenFOAM: A computational approach for efficient and accurate simulations. Int J Thermofluids. 2024;22:100654.
[14] Kamma P, Suvanjumrat C. Assessment of partially premixed flame by in-situ adaptive reduced mechanisms in OpenFOAM. Int J Automot Mech Eng. 2021;18(4):9220–9229.
[15] Yadav DS, Khan A, Paul B, Paul AR. Performance analysis of mixed fuel biogas and LPG in domestic cook stove burner. Int J Creat Res Thought. 2022;10(1):31–35.
[16] Goldmann A, Dinkelacker F. Experimental investigation and modeling of boundary layer flashback for non-swirling premixed hydrogen/ammonia/air flames. Combust Flame. 2021;226:362–379.